Open Access
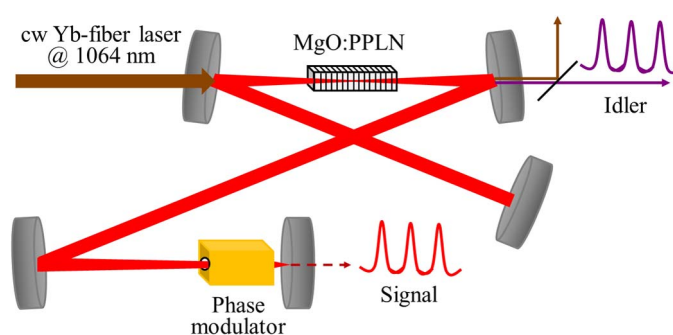
Phase-Modulation-Mode-Locked Continuous-Wave MgO:PPLN Optical Parametric Oscillator

Kavita Devi
S. Chaitanya Kumar
M. Ebrahim-Zadeh

Phase-Modulation-Mode-Locked Continuous-Wave MgO:PPLN Optical Parametric Oscillator

Kavita Devi,[1] **S. Chaitanya Kumar,**[1] **and M. Ebrahim-Zadeh**[1,2]

[1]ICFO-Institut de Ciencies Fotoniques, 08860 Castelldefels, Spain
[2]Institucio Catalana de Recerca i Estudis Avancats (ICREA), 08010 Barcelona, Spain

Abstract: We report phase-modulation mode-locking of a continuous-wave (cw) singly-resonant optical parametric oscillator (OPO) in the near- and mid-infrared based on MgO-doped periodically poled $LiNbO_3$ (MgO:PPLN) and pumped by an Yb-fiber laser at 1064 nm. By investigating the spectral output and pulse formation characteristics of the OPO, we observe a clear transition from an unstable spectrum in cw operation to a stable and smooth profile under phase modulation, confirming mode-locked operation. Pulse generation and spectral characteristics under different operating conditions are studied, including the effects of the location of the intracavity phase modulator and the number of oscillating modes on mode-locked output pulse duration.

Index Terms: Optical parametric oscillators, mode-locked lasers, near- and mid-infrared sources, nonlinear optics and devices.

1. Introduction

For many years, mode-locking techniques in lasers have been exploited for the generation of ultrashort optical pulses [1]. From active to passive, various methods have been studied and demonstrated. Given the broad fluorescence bandwidths in the Ti:sapphire gain medium, over the past two decades, the Kerr-lens-mode-locked (KLM) Ti:sapphire laser [2] has been established as the workhorse of ultrafast science and technology, capable of providing ultrashort pulses with wavelength tuning in the near-infrared (near-IR) [3]. Mode-locked laser sources such as Yb, Er, and Tm fiber lasers, and Cr-doped ZnSe lasers have also been developed providing tuning capability in specific spectral regions in the near-IR to mid-IR [4].

For continuous and broad coverage in arbitrary wavelength regions, nonlinear frequency conversion techniques offer a highly attractive approach to overcome the spectral limitations of lasers [5]. In particular, optical parametric oscillators (OPOs) represent versatile and practical sources of tunable coherent radiation from the ultraviolet to the mid-IR, operating in all temporal domains from the continuous-wave (cw) to femtosecond time-scales [6]. For the generation of ultrashort pulses in the spectral regions covering the ultraviolet to the mid-IR, in particular,

synchronously-pumped OPOs are now established as viable tunable ultrafast sources [7]. However, OPOs based on synchronous pumping require the deployment of mode-locked ultrafast lasers as the pump source, thus generally resulting in relatively high complexity, large size, and high cost for such OPOs. To overcome the requirement for ultrafast pump lasers, in recent years, the possibility of direct application of mode-locking methods to OPOs under cw pumping has been experimentally investigated [8]–[12]. For OPOs, it was shown earlier [13] that synchronous pumping is the only option for generating ultrashort pulses, because a parametric device is not able to store the pump energy for use at later times. However, the advent of quasi-phase-matched (QPM) materials has enabled the possibility of active mode-locking in cw-pumped OPOs. In recent years, different QPM materials have been exploited, enabling direct active mode-locking of cw OPOs, generating steady-state pulses in the near-IR. As known, the active mode-locking technique can be achieved using amplitude or frequency modulation. Based on acousto-optic or electro-optic elements, mode-locking has been demonstrated in various earlier reports on lasers [14]–[17].

Over the past few years, using an acousto-optic modulator (AOM), a cw-pumped OPO based on MgO-doped periodically-poled LiNbO$_3$ (MgO:PPLN), in doubly-resonant oscillator (DRO) and singly-resonant oscillator (SRO) configurations has been demonstrated to generate stable nanosecond pulses [8], [9]. In addition, passive mode-locking has been theoretically studied in a pump-swept OPO [18]. In one recent demonstration, by using electro-optic phase modulation, and by deploying a cw green laser at 532 nm to pump a cw SRO based on MgO:sPPLT, we reported the generation of picosecond pulses in the near-IR [11]. In addition, deploying the same laser source and nonlinear material, we have demonstrated direct active phase-modulation mode-locking of a cw DRO operating near degeneracy at 1064 nm [12]. Given the higher passive spectral and temporal stability in a SRO compared to DRO, here we study the operating characteristics of a cw SRO based on MgO:PPLN as the nonlinear material pumped by a cw Yb-fiber laser at 1064 nm, which uses an electro-optic modulator (EOM) as a single mode-locking element, and we demonstrate the possibility to achieve mode-locking at longer wavelengths into the near- and mid-IR. Since the basis for achieving mode-locked output is to induce a constant phase relation between the modes in the resonant cavity, as in a conventional mode-locked laser, the Fourier relation between the frequency and time domain predicts the shortest attainable pulse duration for a given spectral output. Therefore, it provides useful information about the strategies that need to be implemented in order to ultimately achieve transform-limited output performance from the device. As such, it is important to study the frequency domain behavior and the spectral output from cw mode-locked OPOs to gain further insight into the pulse formation mechanisms and spectral properties. In this study, we thus also explore the spectral output and pulse formation in the directly phase-modulation mode-locked MgO:PPLN cw SRO operating in a different spectral range in near- and mid-IR, and under a different pumping level from our previous report [11].

2. Experimental Setup Details

The cavity configuration for the mode-locked cw SRO is similar to that in our earlier work [11], and is shown in Fig. 1. The pump source is a cw Yb-fiber laser (IPG Photonics, YLR-30-1064-LP-SF), delivering up to 30 W of output power at 1064 nm in a single-frequency, linearly-polarized beam with $M^2 \sim 1.01$ and a nominal linewidth of 89 kHz. The SRO is configured in a standing-wave cavity comprising two concave mirrors, M_1 and M_2 ($r = 150$ mm), a third concave mirror, M_4 ($r = 500$ mm), and two plane mirrors, M_3 and M_5. Mirrors, M_{1-5}, are highly reflecting for the signal ($R > 99\%@1.3$–1.9 μm), and transmitting for the idler ($T > 90\%@2.2$–4 μm) and pump ($T > 92\%@1064$ nm). The nonlinear crystal is a 48-mm-long, 6.2-mm-wide and 1-mm-thick, 5% bulk MgO:PPLN, which is housed in an oven with a stability of ± 0.1 °C. The crystal contains five gratings with periods ranging from $\Lambda = 29.5$ μm to $\Lambda = 31.5$ μm, in steps of 0.5 μm. However, we only use the $\Lambda = 30$ μm grating period in this study, providing a theoretical wavelength tuning range of 3625-3351 nm for the idler and 1506–1559 nm for the signal by varying the crystal temperature from 25 °C to 200 °C. A lens of focal length,
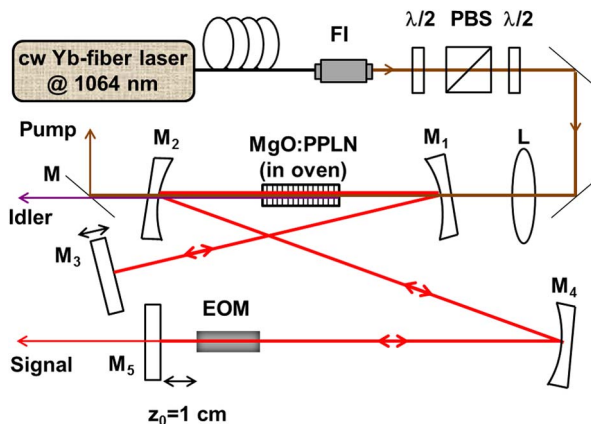
Fig. 1. Schematic of experimental setup. FI, Faraday isolator; $\lambda/2$, half-wave plate; PBS, polarizing beam-splitter, L, lens; M_{1-5}, cavity mirrors; M, dichroic mirror; EOM, electro-optic phase modulator.

$f = 250$ mm, was used to focus the pump beam to a waist radius of $w_{0p} = 63$ μm, resulting in a signal beam waist radius of $w_{0s} = 79$ μm at the center of the crystal. The EOM used is based on a 40-mm-long MgO:LiNbO$_3$ crystal (New Focus, model 4003), with a resonant frequency of $\nu = 80$ MHz and tunability of ± 5 MHz, with both faces antireflection-coated over 1–1.6 μm. It has a 2 mm clear aperture, through which the beam diameter can be adjusted using M_4 and is placed close to M_5. The separation between the EOM end-face and M_5 is $z_0 = 1$ cm. M_3 is mounted on a translation stage to enable adjustment of the cavity length for synchronization with the EOM resonant frequency. The total optical length of the SRO cavity, when synchronized with resonant frequency of EOM, is $L = 2L_{linear} = 3.72$ m. A dichroic mirror, M, is used to separate the non-resonant idler from the transmitted pump beam.

3. Results and Discussion

Keeping the crystal temperature at 100 °C, corresponding to an idler wavelength of 3520 nm (signal at 1525 nm), and without the EOM in the cavity, the MgO:PPLN cw SRO provides an idler power of 3.9 W for 28.7 W of pump power, and has an oscillation threshold of 12.5 W. With the insertion of the EOM into the cavity, the oscillation threshold increases to 16 W and the cw SRO provides 2.5 W of idler power for an input pump power of 28.7 W. The increase in threshold power is attributed to the EOM insertion loss. At 1525 nm, the single-pass insertion loss of the EOM is measured to be $\sim 5\%$ (-0.23 dB). Maintaining the crystal temperature at 100 °C, we investigated mode-locking of the SRO.

3.1. Pulse Width and Stability

We monitored the temporal output of the SRO using an InGaAs photo-detector (20 GHz, 18.5 ps) and a fast oscilloscope (3.5 GHz, 40 GS/s). With fine adjustment of EOM modulation frequency and systematic change in the modulation depth, we obtained sharp pulses with duration of 305 ps and 236 ps at 160 MHz and 80 MHz, as shown in Fig. 2(a) and (b), respectively. The 80 MHz pulse train recorded in the microsecond scale, depicting the intensity noise on the output pulses, is shown in Fig. 2(c), where a pulse peak-to-peak stability better than 7% is measured over 100 μs.

3.2. RF Measurements

We also characterized the mode-locked pulses by performing RF spectral measurements. The wide-span frequency spectrum measurements up to 1.2 GHz for 160 MHz pulses and up to 600 MHz for 80 MHz pulses, obtained by keeping EOM modulation depth at 1.83 rad and tuning modulation frequency to ν and $\nu \pm \Delta\nu$, respectively, are shown in Fig. 3(a) and (b). Here, ν is
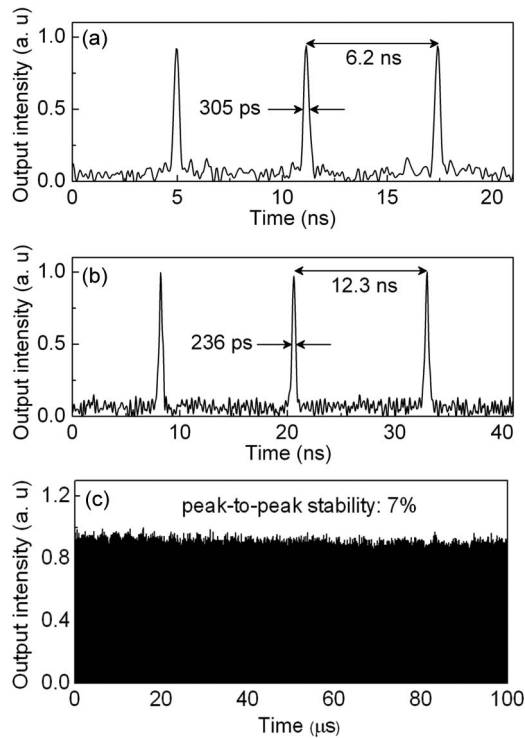
Fig. 2. Pulse train obtained at (a) 160 MHz and (b) 80 MHz. (c) Output pulse train at 80 MHz over 100 μs.
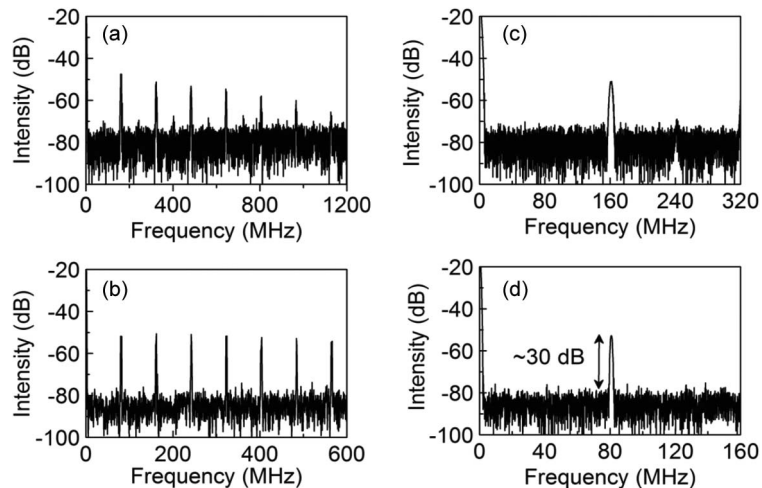
Fig. 3. Wide-span RF spectrum for (a) 160 MHz pulses and (b) 80 MHz pulses. RF spectrum measured around the fundamental repetition rate for (c) 160 MHz pulses and (d) 80 MHz pulses with resolution bandwidth of 3 MHz.

$\sim$80 MHz, and $\Delta\nu$ is a small change in modulation frequency on either side of ν, which is of the order of kHz. In Fig. 3(b) the repetition rate of 80 MHz and its harmonics are seen as sharp peaks, with no significant spectral modulation, implying negligible instabilities. Fig. 3(c) and (d) show the RF spectrum around the fundamental repetition rate for 160 MHz and 80 MHz pulses, respectively. As can be seen, for 80 MHz pulses, peak-to-background ratio of $\sim$30 dB has been obtained.
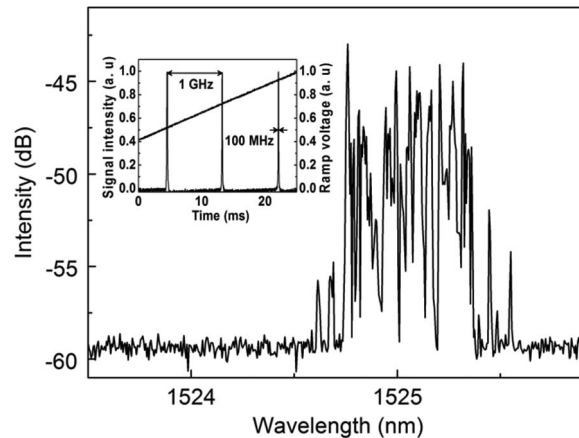
Fig. 4. Output signal spectrum with SRO under cw operation. (Inset) Single-frequency spectrum of signal output.
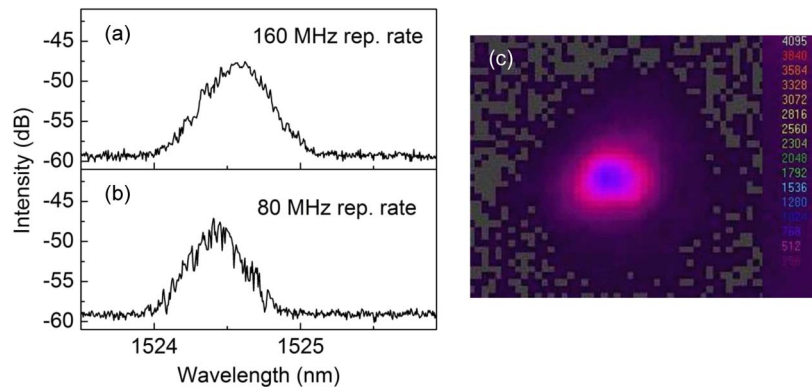

Fig. 5. Output signal spectrum under mode-locked conditions at (a) 160 MHz and (b) 80 MHz. (c) Spatial beam profile of the mode-locked signal pulses at 80 MHz.

3.3. Spectral Measurements and Beam Quality

In order to study mode-locking in the frequency domain, we performed spectral measurements for different SRO operating conditions. Fig. 4 shows the signal spectrum, recorded using optical spectrum analyzer (OSA), with a resolution of 0.05 nm, when the EOM is switched off, and the OPO is under cw operation. As seen, the output spectrum is not smooth, and exhibits a bandwidth of 0.8 nm. This indicates the occurrence of mode hops in the SRO cavity. Given the signal acceptance bandwidth of 2 nm for the 48-mm-long MgO:PPLN crystal, the mode hopping could be attributed to thermal fluctuations and mechanical vibrations of the OPO cavity. However to confirm the instantaneous single-frequency operation of the SRO, we recorded the transmission spectrum of the signal output under cw condition, using a confocal Fabry–Perot interferometer, FPI (FSR = 1 GHz, finesse = 400). The transmission spectrum confirms single-frequency operation with an instantaneous linewidth of $\sim$100 MHz, as shown in the inset of Fig. 4. Keeping the modulation depth fixed at 1.83 rad and tuning the modulation frequency to $\nu \sim 80$ MHz, when sharp pulses at 160 MHz are observed, using an OSA with identical instrument settings as that in the cw measurements, we then recorded the output pulse signal spectrum. The results are shown in Fig. 5. As can be seen in Fig. 5(a), the output spectrum becomes smooth and forms an envelope under phase-modulation. Fig. 5(b) shows the spectral output for 80 MHz pulses when the modulation depth is again kept fixed at 1.83 rad and modulation frequency is detuned to $\nu \pm \Delta\nu$. Again, the output spectrum is seen to form an envelope with a FWHM bandwidth of $\sim$0.52 nm corresponding to 835 axial modes of the OPO cavity. The
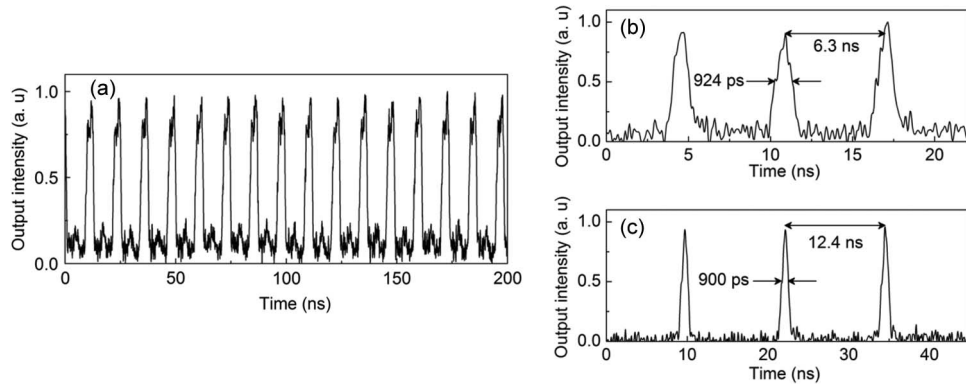
Fig. 6. (a) Output in time domain when etalon is incorporated at AOI = 0° and modulation depth and frequency kept at 1.63 rad and $\nu \pm \Delta\nu$, respectively. Pulse train obtained for z_0 = 10 cm at (b) 160 MHz and (c) 80 MHz.

transition from a modulated spectrum under cw operation to a smooth profile under phase modulation is clear indication of locking of the OPO cavity modes, resulting in pulsed output generation. We have also observed that when the SRO is mode-locked, the spectrum is shifted by $\sim$0.5 nm towards shorter wavelengths, as compared to cw operation. We believe this shift could be due to the group velocity dispersion that persists between the interacting waves for broad bandwidth signal under mode-locked operation [19]. However, to fully understand this effect, further study is needed. Another contributing factor for this wavelength shift could be the thermal load of the nonlinear crystal, resulting in a rise in crystal temperature, and thus a longer signal wavelength in MgO:PPLN under cw operation [20]. The shift in output wavelength during the transition from cw to mode-locked operation was also observed using a conventional spectrum analyzer with low resolution. In addition, the signal transmission spectrum in mode-locked operation, when observed using the same FPI, showed some indistinct broadening, as also noted in our previous work [11]. However, limited by the available diagnostics, we could not determine the signal spectral bandwidth.

We also measured the far-field energy distribution of the mode-locked signal pulses at 80 MHz. The result is shown in Fig. 5(c), confirming a TEM_{00} spatial profile with a beam circularity > 90%.

3.4. Cavity Axial Modes and Position of EOM

At maximum pump power, when the OPO is operating $\sim$1.8 times above threshold, it is possible to study the effect of number of oscillating cavity modes on mode-locking by performing frequency selection using an etalon. For the etalon, we used a 0.4-mm-thick uncoated fused silica plate (FSR = 255 GHz, finesse < 1), which was inserted between mirrors M_2 and M_4. Under cw operation, with the EOM off, we recorded the output spectrum at different angle of incidence (AOI) on the etalon, and observed that the central wavelength shifts from 1525 nm at AOI = 0° to 1524.3 nm at AOI = 3°. To explore the role of the number of oscillating cavity modes in mode-locking, we monitored the output in the time domain while incorporating the etalon at AOI = 0° under cw condition. To achieve mode-locking, we increased the modulation depth to 1.63 rad and tuned modulation frequency to $\nu \pm \Delta\nu$. Fig. 6(a) shows the temporal output. As evident, we did not observe clear pulse formation. However, indistinct pulses at 80 MHz with 3.1 ns duration were obtained. This is attributed to the reduced number of available cavity modes that can be phase-locked, resulting in less efficient mode-locking and longer output pulses. With further increase in the modulation depth beyond 1.63 rad, the OPO operation was observed to cease. At other AOI on etalon, mode-locking was not achieved. In such situations the OPO ceased operation after even a small increase in modulation depth from minimum.

In a recent report on actively mode-locked DRO, pumped at 532 nm, where a broad spectral bandwidth is available near degeneracy, we demonstrated the dependence of output pulse

duration on the position of EOM in the cavity [12]. To study this dependence in the present SRO, we increased the separation of the EOM from mirror, M_5, from $z_0 = 1$ cm to $z_0 = 10$ cm, and observed the OPO output in the time domain. The general behavior of the temporal output is similar to that when EOM is placed close to M_5 ($z_0 = 1$ cm). However, we observed significant difference in the pulse duration. Fig. 6(b) and (c) show the pulses obtained for $z_0 = 10$ cm at 160 MHz and 80 MHz, respectively. As evident, the pulse duration for 160 MHz and 80 MHz is 924 ps and 900 ps, respectively, which are $\sim$three to four times longer than the pulse durations obtained for $z_0 = 1$ cm.

4. Conclusion

We have demonstrated a phase-modulation-mode-locked cw SRO in the near-and mid-IR based on MgO:PPLN, and have investigated its spectral and pulse formation characteristics. We have observed a clear transition from an unstable spectrum in cw operation to a stable spectrum with smooth profile under phase-modulation, clearly confirming mode-locked operation. We have also studied the effect of number of oscillating modes and the position of phase modulator on the duration of the output pulses. The results clearly confirm the expected Fourier transform relationship between spectral and temporal characteristics of the mode-locked OPO. The shortest mode-locked pulse length of 236 ps so far generated is far from transform-limited duration of 6.6 ps for the available spectral bandwidth of $\sim$0.52 nm (FWHM), which indicates that the contributing bandwidth to mode-locking is narrow. This is attributed to the large intracavity group velocity dispersion (GVD) in the 48-mm-long MgO:PPLN and 40-mm-long LiNbO$_3$ modulator crystals, which in total amount to $+9530$ fs^2 ($+108.3$ fs^2/mm), as well as the GVD of the OPO cavity mirrors and crystal coatings, which is unknown. With careful intracavity GVD control using negatively chirped OPO mirrors, substantially shorter mode-locked output pulses approaching the transform limit are expected. Further reductions in pulse duration can also be achieved using higher modulation frequencies for the EOM with suitable thermal management. It is also to be noted that while the present study relates to the mode-locked signal pulses, due to the lack of diagnostics in the idler wavelength range, we expect the same general behavior of the idler pulses, as already confirmed in our earlier studies [11]. This study also demonstrates that the phase-modulation mode-locking technique for the generation of optical pulses can be deployed in different spectral regions using cw OPOs based on different nonlinear materials and pump sources.

Acknowledgment

References

[1] H. A. Haus, "Mode-locking of lasers," *IEEE J. Sel. Top. Quantum Electron.*, vol. 6, pp. 1173–1185, Nov./Dec. 2000.
[2] C. G. Durfee *et al.*, "Direct diode-pumped Kerr-lens mode-locked Ti:sapphire laser," *Opt. Express*, vol. 20, no. 13, pp. 13 677–13 683, 2012.
[3] S. Chaitanya Kumar, G. K. Samanta, K. Devi, S. Sanguinetti, and M. Ebrahim-Zadeh, "Single-frequency, high-power, continuous-wave fiber-laser-pumped Ti:sapphire laser," *Appl. Opt.*, vol. 51, no. 1, pp. 15–20, Jan. 2012.
[4] I. T. Sorokina and E. Sorokin, "Femtosecond Cr^{2+}-based lasers," *IEEE J. Sel. Top. Quantum Electron.*, vol. 21, no. 1, Jan./Feb. 2015, Art. ID. 1601519.
[5] M. Ebrahim-Zadeh and I. T. Sorokina, Eds., *Mid-Infrared Coherent Sources and Applications*, 1st ed. Houten, The Netherlands: Springer-Verlag, 2007.
[6] M. Ebrahim-Zadeh, *Topics in Applied Physics*, I. T. Sorokina and K. L. Vodopyanov, Eds. Berlin, Germany: Springer-Verlag, 2003, pp. 179–218.
[7] M. Ebrahim-Zadeh, "Efficient ultrafast frequency conversion sources for the visible and ultraviolet based on BiB$_3$O$_6$," *IEEE J. Sel. Top. Quantum Electron.*, vol. 13, no. 3, pp. 679–691, May/Jun. 2007.
[8] N. Forget, S. Bahbah, F. Bretenaker, M. Lefebvre, and E. Rosencher, "Actively mode-locked optical parametric oscillator," *Opt. Lett.*, vol. 31, no. 7, pp. 972–974, Apr. 2006.
[9] J.-M. Melkonian *et al.*, "Active mode locking of continuous-wave doubly and singly resonant optical parametric oscillators," *Opt. Lett.*, vol. 32, no. 12, pp. 1701–1703, Jun. 2007.

[10] A. Esteban-Martin, G. K. Samanta, K. Devi, S. Chaitanya Kumar, and M. Ebrahim-Zadeh, "Frequency-modulation-mode-locked optical parametric oscillator," *Opt. Lett.*, vol. 37, no. 1, pp. 115–117, Jan. 2012.

[11] K. Devi, S. Chaitanya Kumar, and M. Ebrahim-Zadeh, "Mode-locked, continuous-wave singly resonant optical parametric oscillator," *Opt. Lett.*, vol. 37, no. 18, pp. 3909–3911, Sep. 2012.

[12] K. Devi, S. Chaitanya Kumar, and M. Ebrahim-Zadeh, "Directly phase-modulation-mode-locked doubly-resonant optical parametric oscillator," *Opt. Express*, vol. 21, no. 20, pp. 23 365–23 375, Oct. 2013.

[13] M. Becker, D. Kuizenga, D. Phillion, and A. Siegman, "Analytic expressions for ultrashort pulse generation in mode-locked optical parametric oscillators," *J. Appl. Phys.*, vol. 45, no. 9, pp. 3996–4005, 1974.

[14] G. W. Hong and J. R. Whinnery, "Switching of phase-locked states in the intracavity phase-modulated He-Ne laser," *IEEE J. Quantum Electron.*, vol. QE-5, no. 7, pp. 367–376, Jul. 1969.

[15] G. T. Maker and A. I. Ferguson, "Frequency-modulation mode locking of a diode-pumped Nd:YAG laser," *Opt. Lett.*, vol. 14, no. 15, pp. 788–790, Aug. 1989.

[16] D. W. Hughes, J. R. M. Barr, and D. C. Hanna, "Mode locking of a diode-laser-pumped Nd:glass laser by frequency modulation," *Opt. Lett.*, vol. 16, no. 3, pp. 147–149, Feb. 1991.

[17] R. P. Scott, C. V. Bennett, and B. H. Kolner, "AM and high-harmonic FM laser mode locking," *Appl. Opt.*, vol. 36, no. 24, pp. 5908–5912, Aug. 1997.

[18] J. Khurgin, J-M. Melkonian, A. Godard, M. Lefebvre, and E. Rosencher, "Passive mode locking of optical parametric oscillators: An efficient technique for generating sub-picosecond pulses," *Opt. Express*, vol. 16, no. 7, pp. 4804–4818, Mar. 2008.

[19] A. Picozzi and P. Aschieri, "Influence of dispersion on the resonant interaction between three incoherent waves," *Phys. Rev. E*, vol. 72, no. 4, Oct. 2005, Art. ID. 046606.

[20] S. Chaitanya Kumar, R. Das, G. K. Samanta, and M. Ebrahim-Zadeh, "Optimally-output-coupled, 17.5 W, fiber-laser-pumped continuous-wave optical parametric oscillator," *Appl. Phys. B*, vol. 102, no. 1, pp. 31–35, Jan. 2011.